[5] McElman, J. A., Mikulas, M. M., and Stein, M., "Static and Dynamic Effects of Eccentric Stiffening of Plates and Cylindrical Shells," *AIAA Journal*, Vol. 4, No. 5, May 1966, pp. 887–894.

[6] Wang, C. T., *Applied Elasticity*, McGraw-Hill, New York, 1953.

[7] Zienkiewicz, O. C. and Cheung, Y. K., *The Finite Element Method in Structural and Continuum Mechanics*, McGraw-Hill, London, 1967.

[8] Hurty, W. C. and Rubinstein, M. F., *Dynamics of Structures*, Prentice-Hall, Englewood Cliffs, N. J., 1965.

[9] Rubinstein, M. F., *Matrix Computer Analysis of Structures*, Prentice-Hall, Englewood Cliffs, N. J., 1967.

[10] Kapur, K. K. and Hartz, B. J., "Stability of Plates Using the Finite Element Method," *Journal of the Engineering Mechanics Division*, ASCE, Vol. 92, No. EM2, April 1966, pp. 177–195.

[11] Rubinstein, M. F. and Rosen, R. R., "Dynamic Analysis by Matrix Decomposition," *Journal of the Engineering Mechanics Division*, American Society of Civil Engineers, Vol. 94, No. EM2, April 1968, pp. 385–395.

[12] Timoshenko, S. P. and Gere, J. M., *Theory of Elastic Stability*, 2nd ed., McGraw-Hill, New York, 1961.

NOVEMBER 1970 J. SPACECRAFT VOL. 7, NO. 11

Waffle Plates with Multiple Rib Sizes: II. Design Examples

LAWRENCE D. HOFMEISTER*
TRW Systems, Redondo Beach, Calif.

AND

LEWIS P. FELTON†
University of California, Los Angeles, Calif.

The efficiency of minimum-weight designs of waffle plates having two rib sizes in each stiffening direction is investigated. A wide variety of configurations are examined, including orthogonal and three-way stiffening patterns. Formulations allow multiple independent general in-plane loads. The design problem is expressed as an inequality-constrained minimization problem, and solved using an interior penalty function optimization algorithm. Designs for plates with only one level of stiffeners agree favorably with results of other studies. For these same examples, incorporation of a second rib size is shown to result in major reductions in required weight. Detailed studies of square plates under uniaxial and equal biaxial loads show that waffle plates with two sizes of ribs compare more favorably to sandwich plates than those with a single stiffener size.

Nomenclature

a,b	=	plate length in the x and y directions, respectively
C	=	constant
D	=	$Et^3/12\ (1 - \nu^2)$ = skin bending stiffness
d	=	spacing of primary (smaller) ribs in x direction
d_x,d_y	=	spacings of secondary (larger) ribs
E	=	Young's modulus
$g_i(\mathbf{X})$	=	constraints
h_1,h_2	=	height of primary and secondary ribs, respectively
$N_i(\mathbf{X})$	=	critical loads
N	=	applied load
$Q(\mathbf{X},\mathbf{X})^{(k)}$	=	penalty function
t	=	skin thickness
t_1,t_2	=	thickness of primary and secondary ribs, respectively
u,v,w	=	plate displacements in x, y, and z directions, respectively
$W(\mathbf{X})$	=	plate weight
$\mathbf{X}$	=	vector of design variables
ν	=	Poisson's ratio
ρ	=	material density
σ	=	stress
σ_y	=	yield stress

Received June 22, 1970. This work was partially supported by Grant NsG-423 from NASA to the late F. R. Shanley, Professor of Engineering, University of California, Los Angeles. The authors wish to acknowledge the fact that the structural concept investigated in this paper originated with him.

* Member of the Technical Staff; formerly Postgraduate Research Engineer, University of Calif., Los Angeles, Calif.

† Assistant Professor of Engineering. Member AIAA.

Introduction

RESULTS of an initial study showing the favorable relative efficiencies of waffle plates with multiple sizes of stiffening ribs have been previously reported.[1] This initial study was confined to uniaxially loaded plates containing orthogonal stiffening patterns of the types illustrated schematically in Figs. 1g–j.

The stability analysis formulated in Ref. 1 has been subsequently extended and refined[2] to accommodate general biaxial loading conditions, coupled plate bending and stretching, and equilateral stiffening configurations of the types shown in Figs. 1c and 1k. This improved formulation makes possible more extensive investigation of the efficiency of the multiple-rib-size concept, the results of which are detailed herein.

Design Problem

In this investigation, the minimum-weight design of simply supported rectangular plates having two "levels" of stiffeners and subjected to multiple independent in-plane loads will be considered. Behavior will be assumed to be elastic, with limitations imposed by the possibility of buckling below or at the yield stress σ_y. Modulus of elasticity E, Poisson's ratio ν, material density ρ, plate dimensions a and b, and magnitudes and directions of the applied loads will be assumed to be specified. In each case, the primary (smaller) ribs will also be assumed to have identical size and spacing in all orientations. In addition, spacing and location of secondary (larger) ribs will be specified, and the effect of variation of these parameters on the final designs will be determined parametrically.

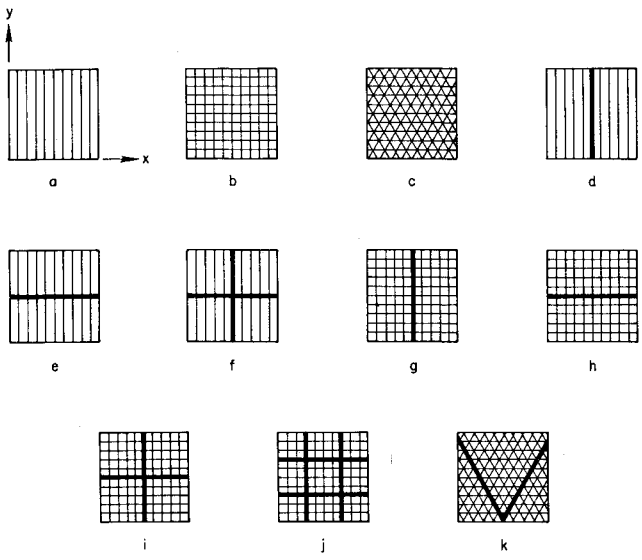

Fig. 1 Stiffening patterns.

The design problem may then be stated in the general form

$$\text{minimize} \quad W(\mathbf{X}) \text{ over } \mathbf{X} \tag{1a}$$

$$\text{such that} \quad g_i(\mathbf{X}) \geq 0 \text{ for all } i \tag{1b}$$

where $W(\mathbf{X})$ is plate weight, $g_i(\mathbf{X})$ are constraints described below, and $\mathbf{X}$ is a solution vector, the components of which are the design variables; i.e.,

$$\mathbf{X}^T = \{t\ d\ t_1\ h_1\ t_2\ h_2\} \tag{2}$$

where t = thickness of plate skin, d = spacing of primary ribs, t_1 = thickness of primary ribs, h_1 = height of primary ribs, t_2 = thickness of secondary ribs, and h_2 = height of secondary ribs.

For plates with orthogonal stiffeners, $W(\mathbf{X})$ is given explicitly by

$$W(\mathbf{X}) \doteq \rho ab\{t + (t_1h_1/d)C_1(\mathbf{X}) + (t_2h_2/ab)[b(a - d_x)/d_x + a(b - d_y)/d_y - t_2(a - d_x)(b - d_y)/d_xd_y]\} \tag{3a}$$

where d_x and d_y are the spacings of the secondary ribs which are oriented parallel to the y and x directions, respectively. The quantity $C_1(\mathbf{X}) = 1.0$ for plates containing uniaxial primary ribs only, and $C_1(\mathbf{X}) = 2 - t_1/d$ for plates with orthogonal primary ribs. Equation (3a) is approximate in that it does not eliminate the small amount of redundant material at the intersections of primary and secondary ribs.

The particular three-way secondary stiffening configuration to be considered is shown in Fig. 1k. The secondary ribs are assumed to extend from the midpoint of one side of a square plate to the corners opposite to it. For this configuration, total plate weight is given by

$$W(\mathbf{X}) \doteq \rho a^2[t + (2t_1h_1/3^{1/2}d)(3 - 2\,t_1/d) + 5^{1/2}\,t_2h_2/a] \tag{3b}$$

There are six distinct limitations on plate behavior which result in constraints on the choice of design variables. Let N be a measure of applied load intensity, and $N_i(\mathbf{X})$ be a measure of critical load intensity. Then, for any design the applied load N must be no greater than 1) the load $N_1(\mathbf{X})$ at which gross buckling of the entire plate occurs, 2) the load $N_2(\mathbf{X})$ at which buckling of the stiffened panels enclosed by secondary ribs occurs, 3) the load $N_3(\mathbf{X})$ at which buckling of unstiffened skin between primary ribs occurs, 4) the load $N_4(\mathbf{X})$ at which buckling of primary ribs occurs, 5) the load $N_5(\mathbf{X})$ at which buckling of secondary ribs occurs, and 6) the load $N_6(\mathbf{X})$ at which the yield stress is reached in either skin or stiffeners.

Thus, "behavioral" constraints can be formulated as

$$g_i(\mathbf{X}) \equiv (N_i(\mathbf{X}) - N)/N \geq 0 \qquad i = 1,\ldots,6 \tag{4}$$

Several additional "side" constraints must also be introduced to assure that designs will be physically realistic.[1] The determination of critical loads $N_i(\mathbf{X})$ is reviewed in the next section.

The optimum plate design is achieved by mathematical programing. An interior penalty function suggested by Fiacco and McCormick[3] is used to transform the inequality-constrained minimization problem, Eqs. (1), into a sequence of unconstrained optimization problems. The penalty function for step $(k + 1)$ in the sequence is given by

$$Q(\mathbf{X},\mathbf{X})^{(k)} = 1/[\mathrm{W}(\mathbf{X}^{(k)}) - \mathrm{W}(\mathbf{X})] + \sum_i [1/g_i(\mathbf{X})] \tag{5}$$

where $\mathbf{X}^{(k)}$ is the result of the previous minimization of step k. An unconstrained minimum of the Q-function is found numerically by searching over the feasible values of $\mathbf{X}$. Under suitable conditions, the sequence of $\mathbf{X}^{(k)}$ thus generated converges to the solution of the originally stated constrained minimization problem. Each unconstrained problem in this sequence is solved using the Variable Metric Method of Fletcher and Powell.[4]

Critical Loads

Solution of the design problem requires that, for any set of design variables, the various critical loads $N_i(\mathbf{X})$ be determined in order to guarantee that constraints (4) are satisfied. Procedures for determining the gross buckling load, $N_1(\mathbf{X})$, have been developed in detail in Ref. 2, and will not be repeated here. In general, it is assumed that the prebuckling and preyielding states are linear, and that the critical loads are independent of one another.

For plates with both primary and secondary ribs, the larger secondary ribs divide the plate into subpanels that are stiffened with only the primary ribs. Since the secondary ribs are locally much stiffer than such panels, the panels can be conservatively assumed to be simply supported along the edges bounded by the secondary ribs.

For plates with one-way and two-way secondary stiffeners, the buckling analysis of the stiffened panels follows directly from that for gross buckling of the entire plate. However, since there are no secondary ribs in such panels, the energy expressions[2] must be modified accordingly. Also, in the energy expressions, d_x and d_y replace a and b, respectively. It must be noted in addition that only a portion of the total in-plane load is distributed to each stiffened panel.

The fact that these panels have no secondary stiffening leads to a considerable reduction in the effort to compute the buckling load $N_2(\mathbf{X})$. The secondary stiffeners force the plate to buckle in a combination of the assumed mode shapes, thus making it necessary to include many such independent shapes in the solution for gross buckling load. However, the stiffened panels enclosed by secondary ribs fail in one mode shape, reducing the stiffness and stability matrices to 3×3's. The buckling load $N_2(\mathbf{X})$ for each assumed mode can then be found in closed form. A number of such modes can be assumed, and that mode that gives the lowest buckling load is the critical buckling shape. Therefore, no time-consuming matrix iteration is necessary to find the critical load.

For the plates with three-way primary and secondary stiffening, the panels reinforced with only primary ribs are equilateral triangles in shape. The strain energy of such panels was derived in detail in Ref. 5, and is based upon the following displacement function taken from Ref. 6

$$w = W_0 \sin(2\pi y/3^{1/2}a)[\cos(2\pi x/a) - \cos(2\pi y/3^{1/2}a)] \tag{6a}$$

Note that the assumed condition of simple supports for the stiffened triangular panels are met by this function, in which

the origin of coordinates has been translated to the intersection of secondary ribs. Symmetrical deflections in stretching were chosen as[5]

$$u = U_0 \sin(2\pi y/3^{1/2}a) \sin(2\pi x/a) \quad (6b)$$

$$v = V_0[\cos(\pi x/a) - \cos(\pi y/3^{1/2}a)] \quad (6c)$$

The first stretching function above provides for a sinusoidal variation of u along the edges $y = -3^{1/2}x$ and $y = 3^{1/2}x$, and zero variation along $y = 3^{1/2}a/2$ and $y = 0$. The second function Eq. (6c) allows a sinusoidal variation of v along the edge $y = 3^{1/2}a/2$. Thus, the shape functions chosen for the triangular panels are analogous to those selected for rectangular panels.[2]

Using the shape functions of Eqs. (6) in the potential energy expression,[2,5] the critical buckling load is

$$N_2(\mathbf{X}) = (K_{11}K_{22}K_{33} + 2K_{12}K_{13}K_{23} - K_{13}^2K_{22} - K_{12}^2K_{33} - K_{11}K_{23}^2)/(K_{11}K_{22}S_{33} - K_{12}^2S_{33}) \quad (7a)$$

where

$$K_{11} = (\pi^2 3^{1/2}/24)[C(7 - \nu) + 5(3^{1/2})A_1] \quad (7b)$$

$$K_{12} = \tfrac{4}{15}[4C(2\nu - 1) - 3^{1/2}A_1] \quad (7c)$$

$$K_{13} = -(\pi^3/a)A_1Z_1 \quad (7d)$$

$$K_{22} = (3^{1/2}\pi^2/48)[C(5 - 3\nu) + 3(3^{1/2})A_1] + (3^{1/2}/12)C(3\nu - 1) \quad (7e)$$

$$K_{23} = -(4\pi 3^{1/2}/225a)A_1Z_1\,(109 + 15\pi) \quad (7f)$$

$$K_{33} = (3^{1/2}\pi^4/3a^2)[8D + 6(3^{1/2})A_1I_1] \quad (7g)$$

$$S_{33} = (3^{1/2}\pi^2/4)n_{2x}(\mathbf{X}) + n_{2y}(\mathbf{X}) \quad (7h)$$

and

$$C = Et/(1 - \nu^2),\ D = Et^3/12(1 - \nu^2),$$

$$A_1 = h_1,\ Z_1 = h_1 + 5$$

$$I_1 = \tfrac{1}{3}h_1^2 + \tfrac{1}{2}h_1t + \tfrac{1}{4}t^2$$

In Eq. (7h), $n_{2x}(\mathbf{X})$ gives the portion of the load applied in the x direction that is transmitted to the stiffened triangular panel, and $n_{2y}(\mathbf{X})$ gives the portion of the load in the y direction transmitted to the panel. These quantities are based upon the equivalent thicknesses of the panel and the entire stiffened plate.

The buckling load $N_3(\mathbf{X})$ of the unstiffened skin between primary ribs follows from the analyses for panel buckling by setting $t_1 = h_1 = 0$, and by replacing stiffened panel dimensions by skin panel dimensions. For simple states of loading, $N_3(\mathbf{X})$ is given explicitly by

$$N_3(\mathbf{X}) = n_3(\mathbf{X})kD[\pi/(d - t_1)]^2 \quad (8)$$

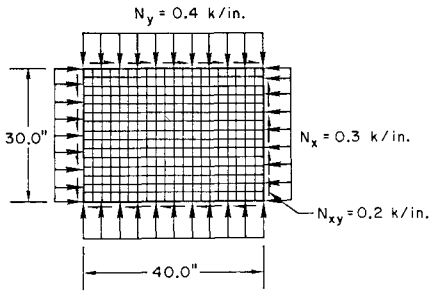

Fig. 2 Design example 1.

where $n_3(\mathbf{X})$ gives the portion of the load transmitted by the skin. For square skin panels $k = 4.0$ for uniaxial compression, $k = 2.0$ for equal biaxial compression, and $k = 9.34$ for pure shear. For equilateral triangular skin panels $k = 9.755$ for uniaxial compression, and $k = 5.333$ for equal biaxial compression.

The critical loads $N_4(\mathbf{X})$ and $N_5(\mathbf{X})$ for primary and secondary ribs correspond to the buckling loads for long uniaxially compressed panels which are simply supported on three edges and free on the fourth (long) edge. This critical load is given by

$$N_i(X) = n_i(X)(\pi/h_j)^2[Et_j^3/12(1 - \nu^2)][(h_j/c_j) + 0.456] \quad (9)$$

where, for primary ribs, $i = 4$ and $j = 1$. For unidirectional stiffening patterns, $c_1 = a$ or b, and for two-way stiffening, $c_1 = (d - t_1)$. In Eq. (9), $n_i(\mathbf{X})$ gives that portion of the load transferred to the stiffener. For secondary ribs, $i = 5, j = 2$, and $c_2 = d_y$ or d_x.

For three-way primary and secondary stiffening configurations, Eq. (9) must be modified slightly since the applied loads are not in the same direction as the ribs.[5]

The Von Mises yield criterion

$$\sigma_y^2 = (\sigma_x^2 - \sigma_x\sigma_y + \sigma_y^2 + \tfrac{3}{2}\sigma_{xy}^2)$$

is used to compute the yielding load $N_6(\mathbf{X})$. Stress components are obtained by dividing applied load by cross-sectional area of the plate.

Examples

Designs were obtained for a wide range of stiffening patterns and load conditions in order to verify the appropriateness of the formulations and evaluate relative efficiency of the structural concept. Detailed analyses were conducted for square plates subjected to uniaxial and equal-biaxial loads, as well as for some rectangular plates subjected to more general load conditions.

Table 1 Design results for examples 1–4

			Variables						Constraints, %							
Example	Design	Weight, lb	t, in.	d, in.	t_1, in.	h_1, in.	t_2, in.	h_2, in.	Load condition	g_1	g_2	g_3	g_4	g_5	g_6
1(Fig.2)	Current	15.38	0.032	2.012	0.176	0.568	...	...	(1)	99.5	...	96.01	.0	...	12.3
	Ref. 7	16.86	0.040	2.534	0.236	0.560	...	...	(1)	100.0	...	70.1	...	...	...
2	Current	161.6	0.042	3.544	0.534	0.458	...	...	(1)	88.2	...	35.8	0.0	...	1.8
									(2)	98.2	...	67.7	0.0	...	20.2
									(3)	99.2	...	69.1	0.0	...	9.8
	Ref. 7	187.2	0.052	3.705	0.642	0.448	...	...	(1)	...	...	...	...	...	...
									(2)	97.5	...	...	...	...	...
									(3)	100.0	...	...	...	...	...
3[a]	Current	7.46	0.034	3.401	0.060	0.566	0.079	1.683	(1)	95.8	20.9	94.6	16.2	86.8	14.6
4[b]	Current	96.62	0.072	3.582	0.183	0.428	0.719	1.045	(1)	64.5	10.0	37.5	0.0	0.0	3.1
									(2)	97.8	16.2	4.6	0.0	0.0	31.5
									(3)	93.1	15.2	64.7	0.0	0.0	15.6

[a] Similar to example 1, except plate contains one central secondary rib in each direction (as in Fig. 1i).
[b] Similar to example 2, except plate contains one central secondary rib in each direction (as in Fig. 1i).

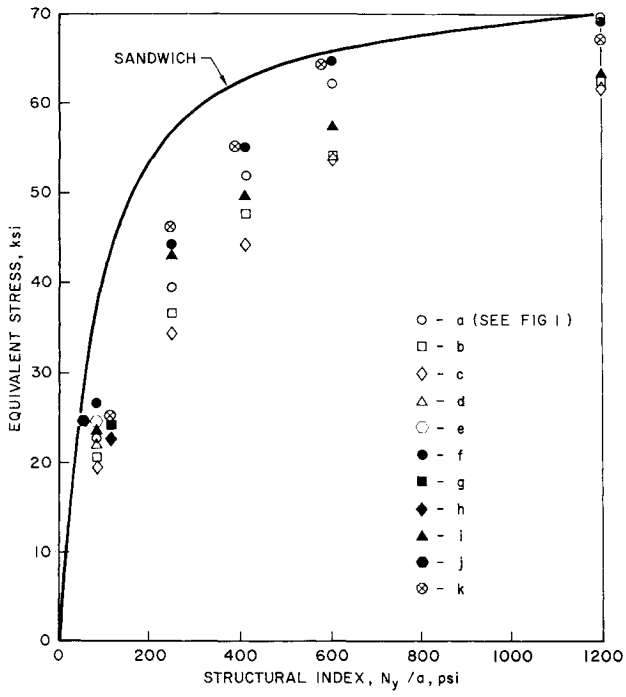

Fig. 3 Optimum stresses for uniaxial loading.

1. Comparison with Other Designs

Figure 2 schematically illustrates dimensions and design loads for a waffle plate which is stiffened by orthogonal primary ribs of uniform size, equally spaced in the x and y directions. This design example was first presented by Schmit et al.[7] Variables for this example are skin thickness t, primary rib spacing d, and thickness t_1. The total depth of the plate (skin plus primary stiffeners) is constrained to equal 0.6 in., so that $h_1 = 0.6 - t$. Material properties are taken as $E = 10.5 \times 10^6$ psi, $\nu = 0.32$, $\sigma_y = 72$ ksi, and $\rho = 0.101$ lb/in^3.

The plate was designed using the formulations contained herein and in Ref. 2, and the results were compared with those of Ref. 7. In Ref. 7, a search technique to find mode shapes for gross and panel buckling was employed in conjunction with an interaction relation to obtain the critical load. Synthesis was accomplished for the inequality-constrained optimization problem by using a steepest descent-alternate step procedure.

Table 1 lists the pertinent quantities for the two plates. It is seen that the designs are essentially similar, both with regard to total weight and magnitude of variables. The differences in these quantities can probably be attributed to differences in the stability analyses of the two formulations.

As indicated in Table 1, for the final design of this study, constraints on both gross buckling and skin buckling are active; i.e., the applied load is 99.5% of the gross buckling load and 96% of the skin buckling load. Although not included in Table 1, results also indicate that the buckled shape of the plate is composed primarily of the term corresponding to $m = n = 1$.

A second example was also taken from Ref. 7. As in the previous case, the plate is assumed to be stiffened by uniform, equally spaced orthogonal primary ribs only. Design conditions, however, include three independent sets of loads. The plate is rectangular with $a = 70$ in., $b = 50$ in., and the loads are defined by (1) $N_x = N_y = 0.3$ k/in. (compression), (2) $N_x = -0.5$ k/in. (tension), $N_x = 0.6$ k/in., $N_{xy} = 1.0$ k/in., (3) $N_x = 1.0$ k/in., $N_{xy} = 0.4$ k/in. This is similar to the example shown in Fig. 4 of Ref. 2, except that design load magnitudes are now specified, and the plate does not contain secondary ribs. For this example, $t + h_1$ is constrained to equal 0.5 in., and material properties are taken as $E = 30 \times 10^6$ psi, $\nu = 0.283$, $\sigma_y = 150$ ksi, and $\rho = 0.276$ lb/in.[3]

Design results are listed in Table 1. Again both designs may be seen to be essentially similar, although differences in weight and variables are somewhat more pronounced than in the previous case. Both plates are constrained by gross buckling in load conditions 2 and 3. The predominant term in the mode shape is that for which $m = 2$ and $n = 1$.

The close correlation of results for these two cases, and the examples contained in Ref. 2 which also substantiate the buckling analysis for plates with discrete ribs, appear to justify reasonable confidence in the appropriateness of all formulations and of the efficiency studies which follow.

2. Extension to Plates with Two Sizes of Ribs

The plates of examples 1 and 2 were redesigned with two distinct sizes of stiffeners in each direction. The primary ribs were again restricted to be uniformly spaced, while the larger secondary ribs were assumed to be centrally located in each case. The resulting stiffening patterns are similar to that shown in Fig. 1i.

Design results for these two cases, denoted as examples 3 and 4, respectively, are also listed in Table 1. It may be seen that the weight of each plate with the multiple sizes of stiffeners is on the order of one-half the weight of the corresponding plate of example 1 or 2 which contains only a single level of rib sizes.

This major improvement in plate efficiency is attributable to the significant influence which the secondary ribs exert on gross buckling load and shape. The buckled shape of each plate is now composed primarily of the terms for which $m = n = 1$ and $m = n = 2$. Nevertheless, as in examples 1 and 2, gross buckling and skin buckling are the predominant critical modes. In both new designs, the quantities $t + h_1$ were kept equal to their previous values.

3. Relative Efficiencies of Square Plates under Uniaxial Compression

As in Ref. 1, designs were obtained for a series of square plates with different arrangements of stiffeners, and subjected to various magnitudes of loading intensity. The "structural index," N_y/a is used as a measure of loading intensity because all geometrically similar plates of identical material which have equal values of index will also have the same "equivalent" stresses. Equivalent stress is defined as $N_y/\bar{t}$, where $\bar{t}$ is the equivalent thickness. A single relationship between index and equivalent stress can thus define all possible optimum designs for any family of geometrically similar plates. This allows meaningful comparison of the relative efficiencies of various rib configurations, as well as comparison of waffle plates with sandwich plates.

This study of the efficiency of uniaxially loaded square plates differs from that contained in Ref. 1 in two major respects. First, the stability analysis uses the improved formulation of Ref. 2, wherein both bending and stretching energy are considered. Second, many more rib configurations are studied. These configurations are shown schematically in Figs. 1a–1k. Of particular importance is the inclusion of the 3-way equilateral rib patterns illustrated in Figs. 1c and 1k.

All designs are for plates of 7075-T6 aluminum alloy, with $E = 10.5 \times 10^6$ psi, $\nu = 0.313$, and $\sigma_y = 72$ ksi. Designs were obtained at five distinct values of structural index: 83 psi, 250 psi, 417 psi, 600 psi, and 1200 psi. Computations were based on dimensions $a = b = 12.0$ in., but as noted previously, results are applicable to all geometrically similar plates subjected to identical loading intensities.

Results are presented in Fig. 3, which shows optimum value of equivalent stress, for each plate configuration, as a function of structural index.

In order to avoid overlapping of the data in Fig. 3, some points are shown displaced horizontally from their proper

locations. Values of design parameters and constraints are not listed here, but are tabulated in Ref. 5.

As was reported in Ref. 1, waffle plates with multiple rib sizes can offer a distinct improvement in efficiency over waffle plates with single rib sizes. Of all configurations evaluated, the stiffening patterns illustrated in Figs. 1f and 1k are seen capable of developing the highest equivalent stresses under uniaxial loading, and consequently correspond to the lightest-weight designs.

It should be noted that not all the configurations of plates with multiple rib sizes shown in Fig. 1 were examined at each value of structural index. Instead, only six of the eleven plates were designed at the four higher values of index. Of the plates with multiple rib sizes, those shown in Figs. 1f, i, and k were selected for detailed examination. This choice was based on the fact that the plates of Figs. 1f and k were slightly superior to all others at $N_y/a = 83$ psi. The plate of Fig. 1i was chosen as typical of intermediate efficiency. The relative efficiencies of the configurations remained fairly consistent at all loading intensities.

The importance of the configurational model to design efficiency is clearly illustrated by Fig. 3. Weight differences of over 30% are possible depending on choice of stiffening pattern. Most surprising, however, is the fact that the plate, which is the least efficient of all when it contains only equilateral primary stiffeners (Fig. 1c), can become the most efficient design when secondary stiffeners are added (Fig. 1k). However, for this type of loading the plates of Figs. 1k and 1f are generally about equal in performance.

Also shown in Fig. 3 is a curve of optimum equivalent stress for uniaxially loaded square honeycomb-core sandwich plates, based on the work of Ref. 7. This is somewhat idealized in that it does not account for weight associated with material used to bond face sheets to the core. Nevertheless, the relative improvement in waffle plate efficiency resulting from the addition of secondary ribs is clearly demonstrated.

4. Relative Efficiencies of Square Plates Under Equal Biaxial Compression

The type of design evaluation performed in the previous section was repeated for equal biaxial loads. The structural index remains appropriate as a basis for comparison. Only four stiffening configurations believed to be most relevant were considered.

Results are shown in Fig. 4, which again illustrates the relative superiority of the plates having two levels of stiffeners. Compared to the plates with single stiffener levels, these are capable of developing equivalent stresses which are from 10% to 20% higher. Specifics of the designs are detailed in Ref. 5.

Figure 4 also contains design results for optimized biaxially loaded sandwich plates‡ based on Ref. 8. As in the previous case, weight of bond material was neglected. The core was also assumed to be isotropic.

In general, it appears that the waffle plates are less efficient in comparison to sandwich plates under biaxial loads than under uniaxial loads. However, the relative performances of similar single and multiply-stiffened waffle plates are about the same for both types of loads.

As was noted in Ref. 1, the stiffening patterns shown in Fig. 1, and evaluated in Figs. 3 and 4 do not necessarily encompass the best possible configurations. Future studies should be directed toward improving design capabilities by increasing the number of variables to include different sizes and spacings of all ribs, rib orientations, and more than two levels of ribs. As these examples demonstrate, the generalized waffle configuration appears capable of approaching the efficiency of sandwich construction.

‡ The authors wish to thank Donald Y. Konishi for specially providing this data.

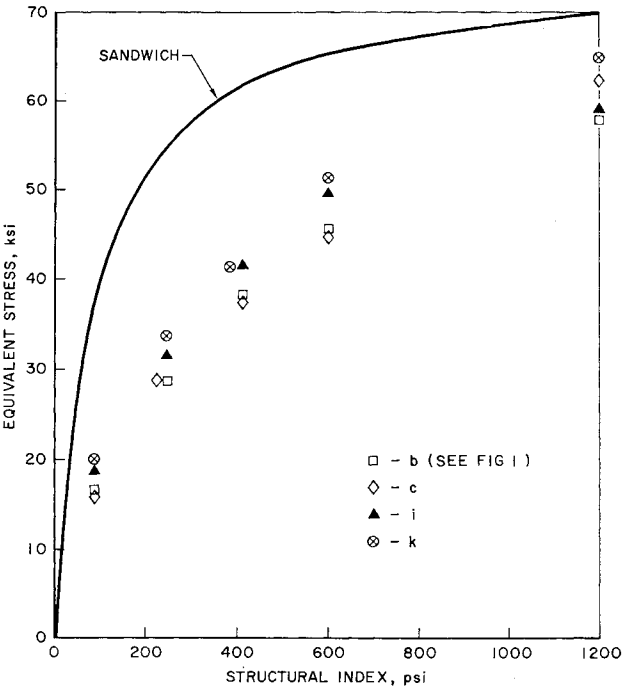

Fig. 4 Optimum stresses for biaxial loading.

References

[1] Hofmeister, L. D. and Felton, L. P., "Synthesis of Waffle Plates with Multiple Rib Sizes," *AIAA Journal*, Vol. 7, No. 12, Dec. 1969, pp. 2193–2199.

[2] Hofmeister, L. D. and Felton, L. P., "Waffle Plates With Multiple Rib Sizes: I. Stability Analysis," *Journal of Spacecraft and Rockets*, Vol. 7, No. 11, Nov. 1970, pp. 1322–1327.

[3] Fiacco, A. V. and McCormick, G. P., "SUMP Without Parameters," Systems Research Memo 121, April 1965, The Technological Institute, Northwestern Univ., Evanston, Ill.

[4] Fletcher, R. and Powel, M. J. D., "A Rapidly Convergent Descent Method for Minimization," *British Computer Journal*, June 1963.

[5] Hofmeister, L. D., "Synthesis of Waffle Plates With Multiple Stiffener Sizes," Ph.D dissertation, Dec. 1968, Dept. of Engineering, Univ. of California, Los Angeles.

[6] Wakasugi, S., "Buckling of Simply Supported Equilateral Triangular Plates," *Bulletin of Japan Society of Mechanical Engineering*, Vol. 4, No. 13, 1961.

[7] Schmit, L. A., Kicher, T. P., and Morrow, W. M., "Structural Synthesis Capability for Integrally Stiffened Waffle Plates," *AIAA Journal*, Vol. 1, No. 12, Dec. 1963, pp. 2820–2836.

[8] Konishi, D. Y., "Optimum Design of a Flat Honeycomb Sandwich Panel Under In-plane Loading," M.S. thesis, 1964, Dept. of Engineering, Univ. of California, Los Angeles.